Local characterization of transmission properties of a two-dimensional photonic crystal

Eric B. McDaniel and J. W. P. Hsu*
Department of Physics, University of Virginia, Charlottesville, Virginia 22901

Lori S. Goldner†
National Institute of Standards and Technology, Gaithersburg, Maryland 20899

R. J. Tonucci‡
Naval Research Laboratory, Washington, DC 20375

Eric L. Shirley and Garnett W. Bryant
National Institute of Standards and Technology, Gaithersburg, Maryland 20899
(Received 15 August 1996; revised manuscript received 15 November 1996)

We use a near-field scanning optical microscope to study optical transmission through a two-dimensional triangular photonic crystal. Spatial variations in the intensity of light coupled through the sample depend on the photon energy and the numerical aperture of the collection optics. We discuss the relationship between the observed dependence and the local structure of the optical modes in the crystal. Features in the data arising from modes with Fourier components inside and outside the first Brillouin zone can be distinguished by this technique. [S0163-1829(97)09816-0]

With the invention of photonic devices, the ability to frequency select and direct light on microscopic length scales is rapidly becoming a reality. One device that has recently attracted much interest is a periodic dielectric structure called a photonic crystal.[1] Spatial periodicity in this device leads, for instance, to coupling of the electromagnetic field modes of neighboring dielectric waveguides. This results in a nontrivial dispersion relation between the energy and wave vector of the allowed modes, i.e., a photonic band structure. Photonic crystals can be designed to transmit or reflect light in a specific range of frequencies,[1] and their properties are tunable by, for example, modification of their periodicity or index of refraction. Defect structures could be designed to introduce impurity bands not only in selected energy ranges, but also in spatial positions. The first demonstration of band-structure effects in photonic crystals was in the mm-wave regime.[2] Since this proof of principle, much research effort has concentrated on making structures for visible and near-infrared light.[1] Recently, photonic band-structure effects in the near-infrared and visible have been measured[3] in two-dimensional (2D) photonic crystals made from nanochannel glass (NCG) arrays.[4]

Photonic crystals have been studied by measuring bulk optical properties such as attenuation and transmission, and band-structure calculations have been used to model and predict these properties.[1] A more detailed understanding can be obtained by studying the microscopic properties such as the local density of photon states and electromagnetic mode structure. Here we demonstrate the use of a transmission-mode near-field scanning optical microscope (NSOM) to measure directly the spatial variations of light coupled through the sample. The resulting optical intensity distributions depend in part on the local mode structure in the photonic crystal.

For a photonic device to be useful at optical frequencies, its lattice spacing must be of the same order as the optical wavelength (λ). Measuring optical properties within a unit cell therefore requires resolution higher than that provided by conventional, far-field, diffraction-limited techniques. In near-field scanning optical microscopy (also NSOM), optical resolution can be better than $\lambda/10$,[5] limited not by λ but rather by the size of the subwavelength aperture used as a probe. In the study of photonic materials, NSOM has been used to measure the local mode structure of optical waveguides with a single or a few propagating modes.[6] Here we study a photonic crystal with many propagating modes. The localized NSOM light contains photons with many transverse momenta, and so enables us to probe modes with different crystal momenta in the photonic crystals. By changing the solid angle of the collection optics, we are able to examine modes with different crystal momenta ($\mathbf{k}$) and Fourier components of total momenta ($\mathbf{q}$).[7] The spatial variations in the intensity of light coupled through the crystal are measured as a function of NSOM probe position, and the relationship between these data and the local electromagnetic mode structure in the 2D crystal is discussed.

The sample studied in this experiment is a NCG array made of two glasses with similar indices of refraction. Details of the fabrication procedure are given in Ref. 4. The array is a 2D triangular lattice of one glass (channel glass) embedded in another glass (matrix glass). The channel glass is cylindrical, approximately 745 nm in diameter ($2r$), with center-to-center nearest-neighbor separation (a) of 1.07 ± 0.05 μm, giving $a/r = 2.87$. The index of refraction of the matrix glass is 1.66, and that of the channel glass is 0.2% to 1.2% higher throughout the visible range.[8] The thickness of the sample is about 250 μm. Figure 1 shows a topographic image taken with a scanning force microscope. The channel glass is depressed slightly, by 3.5 ± 0.5 nm, because it is

 © 1997 The American Physical Society

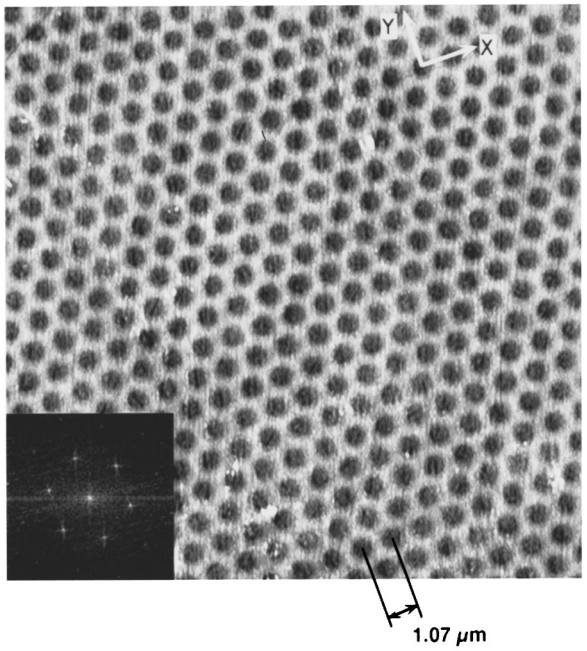

FIG. 1. Topographic image of the NCG sample taken with a scanning force microscope. The image size is 20×20 μm^2. The depressions are 3.5 ± 0.5 nm, and are centered on the channel glass. The inset shows a two-dimensional Fourier transform of a 60×60 μm^2 topographic image.

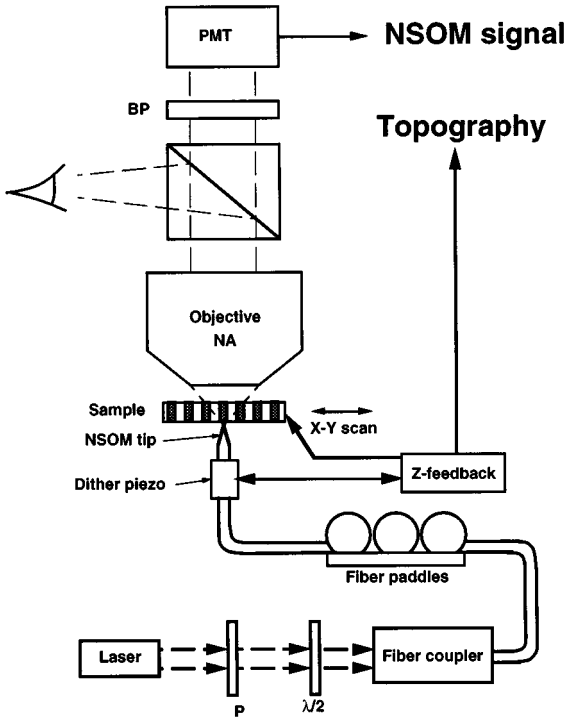

FIG. 2. Schematic of the transmission-mode near-field scanning optical microscope used in this experiment: P, polarizer; $\lambda/2$, half-wave plate; BP, bandpass filter; and PMT, photomultiplier tube. The fiber paddles are used to adjust the polarization of the NSOM light.

preferentially etched during a polishing process. In this paper, the XY plane is the 2D lattice plane, and the Z coordinate is perpendicular to this plane, i.e., along the axis of the channel glass cylinders. The X direction is defined to be parallel to a close-packed direction in the 2D triangular lattice, and the Y direction is perpendicular to X, i.e., in the other high-symmetry direction (see Fig. 1). The reciprocal lattice of a 2D triangular lattice is also triangular with a 30° rotation. The inset in Fig. 1 is a Fourier transform of a larger-scale (60×60 μm^2) topographic image. The $\mathbf{k}=\mathbf{0}$ and first-order reciprocal-lattice points are most prominent, and higher-order points are also evident. The sharpness of these spots indicates that the lattice is well ordered.

A schematic of the experimental setup is shown in Fig. 2. The subwavelength light source is fabricated by tapering and metal coating a single-mode optical fiber so that a small (down to 60 nm) aperture remains at the end. An image is generated as the sample is scanned above the tip of the fiber (NSOM ''probe'' or ''tip''). Contrast in the image is the result of changes in the optical intensity detected by the photomultiplier tube when the tip is at different positions under the sample. Because the angular distribution of light leaving the sample will vary as the sample is moved relative to the tip, the images generated will depend on the collection solid angle of the objective. An important parameter in this study is the numerical aperture (NA) of the collection optics, which is varied between 0.28 and 0.7.[9]

A feedback mechanism is employed to actively maintain the tip at a constant separation from the sample surface in the near field. Nonoptical detection of changes in the shear force[10] is used for this purpose. Topographic and optical transmission images are acquired simultaneously, allowing a correlation between optical features and positions in the NCG lattice. The experiment was performed using two different wavelengths of light: $\lambda=670$ nm, from a diode laser; and $\lambda=488$ nm, from an argon laser. The polarization of the NSOM light can also be controlled and varied.[11]

Periodicity of the NCG permits a description of photonic states in a band-structure picture, wherein the X and Y crystal momentum components [$\mathbf{k}=(k_x,k_y)$]are defined in the first Brillouin zone (BZ) for each mode (in the reduced-zone scheme). Because the index contrast is small, modes are modified only weakly from single plane waves, except near Bragg planes.[12] Photonic band-structure effects have been observed for propagation in the XY plane.[3,13] For propagation along Z (this work), such effects are identified, e.g., by enhanced field strengths observed at channel-glass centers for the lowest-order modes near the zone center. For a given crystal momentum, there will be several propagating modes, each with a different set of Fourier components in various BZ's. The lowest-order mode has its dominant component in the first BZ. The small transverse spatial extent of the NSOM light source corresponds to a wide range of transverse momenta. For a given position of the NSOM probe, NCG modes with the largest amplitude at that position should be most strongly excited. The NA of the collection optics determines which Fourier components of these modes will be present in the signal. The maximum collected $|\mathbf{q}|$ is given by $2\pi(\mathrm{NA})/\lambda$. In this experiment, the reciprocal-lattice distance between the zone center ($\overline{\Gamma}$) and the first BZ boundary ($\overline{X}$) of this 2D photonic lattice is 3.39×10^{-3} nm^{-1}.[14] For 670-nm light, the lowest NA objective selectively collects photons with Fourier components inside the first BZ only. For

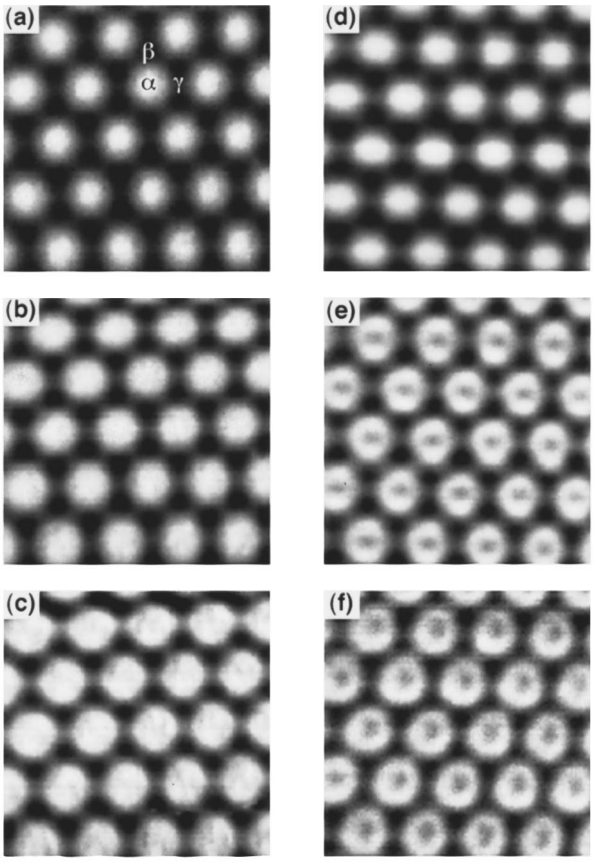

FIG. 3. NSOM images of the NCG arrays. (a)–(c) were taken with a $\lambda=670$ nm diode laser, and (d)–(f) were taken with a blue light argon laser ($\lambda=488$ nm). The collection objective NA in (a) and (d) was 0.28 that in (b) and (d) was 0.55, and that in (c) and (f) was 0.70. The full gray scales represent optical contrast (change in intensity normalized by average intensity) of 53%, 38%, 28%, 54%, 25%, and 15%, respectively in (a)–(f).

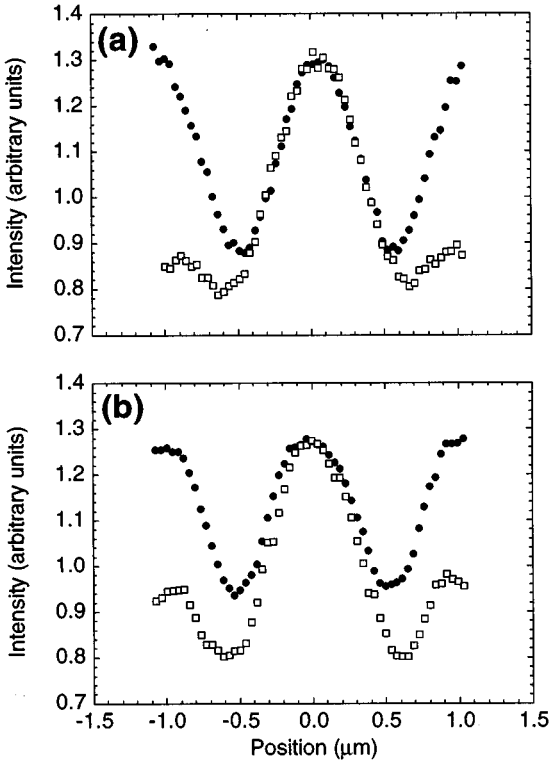

FIG. 4. (a) and (b) Optical intensity change as a function of position in both X (●) and Y (□) directions. Line cuts for $\lambda=670$ nm data, taken from Fig. 3(a), are shown in (a), and similar line cuts for $\lambda=488$ nm data, taken from Fig. 3(d), are shown in (b).

488-nm light, the lowest NA objective collects photons with Fourier components inside and just beyond the first BZ.[15] Therefore the signal for the lowest NA is primarily sensitive to lowest-order modes. Data taken with higher NA detect total momenta farther outside the first BZ,[16] so these data contain information on higher-order modes.

Figure 3 shows NSOM images taken at $\lambda=670$ nm (left column) and $\lambda=488$ nm (right column). Each row corresponds to data taken with a different NA collection objective. The bright spots and ring structures are centered over the depressions that correspond to the center of the channel glass in the topographic image.[17] The NSOM images depend on both the wavelength of light and the objective NA. All data discussed here were taken with NSOM light that is primarily linearly polarized along X. Images taken with Y-polarized light are qualitatively similar. The signal at the channel glass centers [labeled α in Fig. 3(a)] is brighter than at the threefold symmetric (β) and bridge (γ) sites. In all images, the intensity is lowest at β and is intermediate at γ.

In the lowest NA images [Figs. 3(a) and 3(d)], the transmitted intensity is highest when the tip is directly beneath the center of the channel glass, independent of wavelength. Because the low-NA objective collects light with total momenta predominantly inside the first BZ, the images reflect the spatial variations of modes with significant components in this zone, i.e., principally the lowest-order modes (for **k** away from the BZ edge).

As the NA is increased, the overall signal level also increases, as would be expected from a larger collection solid angle. However, the additional signal is not spatially uniform. At higher NA, modes with larger components in higher BZ's contribute to the signal. This includes modes whose maxima occur between lattice sites, so the signal will be relatively larger when the probe is located at these maxima. The specific spatial distribution depends on wavelength. For $\lambda=670$ nm, the bright spots, which are centered on the channels, are larger and display a constant intensity (flat top) across the channel diameter [Figs. 3(b) and 3(c)]. For $\lambda=488$ nm, the signal from channel edges exceeds the signal at channel centers; Figures 3(e) and 3(f) show dark spots near channel centers (ring shape).

Figure 4(a) shows line cuts in both X (close packed) and Y directions for the $\lambda=670$ nm data taken with a 0.28 NA objective. Line cuts for $\lambda=488$ nm data taken under the same condition are shown in Fig. 4(b). The transmitted intensity drops when the tip is between two channels and is lowest at the threefold-symmetric sites. The transmitted intensity at the bridge sites is enhanced for the 488-nm light [Fig. 4(b)] compared to 670-nm light [Fig. 4(a)]. The ratios between measured intensities at channel centers and the threefold sites are 1.60 ± 0.10 and 1.58 ± 0.10,[18] and those between bridges and threefold sites are 1.10 ± 0.04 and 1.18 ± 0.04,[19] for $\lambda=670$ and 488 nm, respectively. We note that the observed large contrast between the channel centers and three-fold

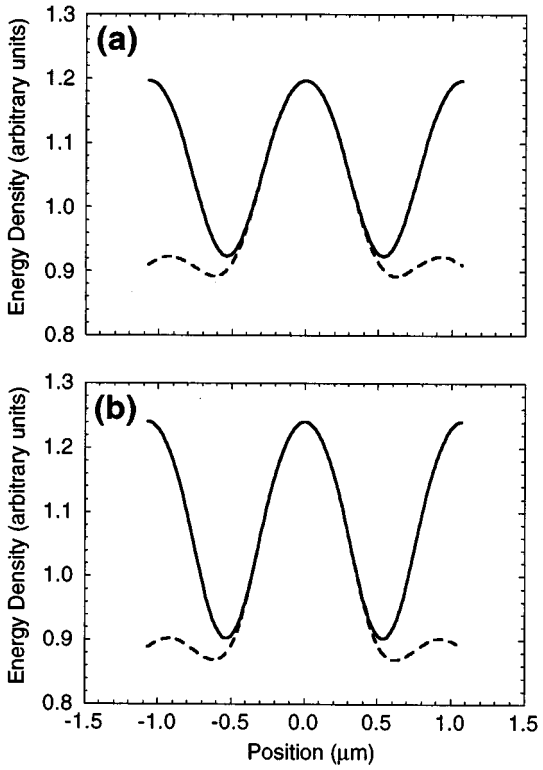

FIG. 5. (a) and (b) Calculations of spatial variations in the lowest mode energy densities in both X (solid line) and Y (dashed line) directions are shown in (a) for $\lambda=670$ nm and (b) for $\lambda=488$ nm.

sites corresponds to an index difference of about 1%.

In this study, we find that images taken with NSOM aperture diameters between approximately 60 and 190 nm display no obvious differences in contrast or resolution. This is not surprising, since the sharpest optical edge observed experimentally[20] was approximately 170 ± 32 nm, even with the smallest diameter tips. The highest Fourier component of the optical modes which is accessible with the 0.7 NA objective corresponds to a length scale of 700 nm. That we see smaller structures indicates that the near-field measurement is sensitive to local changes in optical intensity, with a resolution beyond the diffraction limit. That the smallest structure in this study is 170 nm indicates that this technique should continue to work for crystals with smaller lattice spacing.

As mentioned above, for the lowest NA, the data will be most sensitive to the lowest-order mode at each $\mathbf{k}$ away from the BZ edge. In particular, this data should have a significant contribution from the lowest-order propagating mode at $\mathbf{k}=\mathbf{0}$. Figures 5(a) and 5(b) are solutions of Maxwell's equations for the spatial variations in energy density of this mode at the two wavelengths used. The calculations were polarization averaged and for a crystal with lattice spacing of 1.07 μm, $a/r=2.87$, $n_{\text{matrix}}=1.66$, and $n_{\text{channel}}=1.68$. The calculations show that the lowest-order-mode energy density at $\mathbf{k}=0$ is highest in the channel centers, and lowest, but not zero, in the threefold sites. Moreover, the bridge to threefold intensity ratio is slightly higher for the shorter wavelength, as in the experimental data. However, the calculated intensity ratios between channel centers and threefold sites are 1.34 and 1.43 for $\lambda=670$ and 488 nm, respectively, smaller than the experimentally observed contrasts.

Our NSOM results are a measurement of the transmission properties of the tip-sample system, rather than a direct measurement of the local-energy density. Therefore a more complete model of the transmission process is necessary to extract specific information about the local-mode structure of the crystal. Recently, we began detailed calculations to model directly the images observed here. In our calculations,[21] the tip field is described by the Bethe-Bouwkamp model.[22] Fields inside the NCG are described by the propagating and evanescent bulk modes of that system. Coupling between the tip field and the bulk modes and between the bulk modes and the transmitted field is determined by satisfying the Maxwell boundary conditions. The flux across the plane of the collection optics is determined from the transmitted field. With this model we can determine which optical modes of the bulk NCG are excited by the localized probe field. Preliminary calculations of the small NA images produce line cuts qualitatively similar to those in Figs. 4 and 5.

Experimental results taken with higher NA objectives show two significant differences from the low-NA data. First, overall contrast is reduced as a function of increasing NA (Fig. 3). Second, channel centers are no longer brighter than channel edges. Preliminary calculations for large NA images suggest qualitatively similar results. The overall contrast in the calculated images is reduced as NA is increased. Significant structure appears in the large NA line cuts that is not present at low NA. At large NA, Fourier components in higher Brillouin zones are sampled. We attribute the additional structure in the images to the local structure of higher-order modes that contain these Fourier components. In the calculation, this additional structure is sensitive to index contrast, polarization, BZ sampling, and BZ integration. We are currently completing detailed calculations to identify the modes that determine the structure in the large NA images.

We have demonstrated the sensitivity of our transmission NSOM data to changes in optical photon energy as well as to changes in the NA of the collection optics. NSOM data are expected to vary with the wavelength of the probe light because the dielectric properties of sample depend on wavelength. However, it is often not appreciated that contrast can change with collection angle (or NA). Here we demonstrate that contrast changes dramatically when different regions in photon momentum space are probed. As the NA of collection is increased, the data include contributions from successively higher order modes of the crystal. Calculations of the local-energy density of the lowest-order ($\mathbf{k}=\mathbf{0}$) propagating mode in the photonic crystal and of images as a function of NA support this interpretation. Future theoretical work will provide a more complete analysis that should enable us to extract detailed information about the mode structure and local dielectric constant of the material that otherwise have not been measured.

We thank E. A. Bolden for sample preparation, M. H. Gray for characterization of NSOM apertures, and P.S. Julienne for helpful discussions. E.B. McD. acknowledges financial support from the ONR and J.W.P.H. from Sloan Research. Work done at the University of Virginia was supported by the NSF, and that at NRL was supported by DARPA and ONR.

*To whom correspondence should be addressed. Electronic address: jhsu@virginia.edu
†Electronic address: lori@bruce.nist.gov
‡Electronic address: tonucci@nrl.navy.mil

[1] See for example, J. D. Joannopoulos, R. D. Meade, and J. N. Winn, *Photonic Crystals* (Princeton University Press, Princeton, 1995); or J. Mod. Opt. **41** (1994).

[2] E. Yablonovitch, Phys. Rev. Lett. **58**, 2059 (1987); E. Yablonovitch and T. J. Gmitter, *ibid.* **63**, 1950 (1989); W. M. Robertson *et al.*, *ibid.* **68**, 2023 (1992).

[3] A. Rosenberg *et al.*, Opt. Lett. **21**, 830 (1996); A. Rosenberg, R. J. Tonucci, and E. A. Bolden, Appl. Phys. Lett. **69**, 2638 (1996); H. B. Lin, R. J. Tonucci, and A. J. Campillo, *ibid.* **68**, 2927 (1996); K. Inoue *et al.*, Phys. Rev. B **53**, 1010 (1996).

[4] R. J. Tonucci *et al.*, Science **258**, 783 (1992).

[5] D. W. Pohl, W. Denk, and M. Lanz, Appl. Phys. Lett. **44**, 651 (1984); E. Betzig *et al.*, Science **251**, 1468 (1991).

[6] L. Dhar *et al.*, Proc. SPIE **2535**, 120 (1995); A. G. Choo *et al.*, Appl. Phys. Lett. **65**, 947 (1994).

[7] Both **k** and **q** are two-dimensional vectors in the XY plane.

[8] The indices of the bulk unprocessed glasses were measured by Schott Glass Technologies, Inc., (Ref. 23) at $\lambda=587.6$ nm, and calculated to be 1.657 (matrix) and 1.676 (channel) at $\lambda=670$ nm, and 1.678 (matrix) and 1.689 (channel) at $\lambda=488$ nm. These extrapolated values for the bulk glasses are obtained with an uncertainty of ± 0.001 using a two-constant Cauchy formula [see, for example, F. A. Jenkins and H. E. White, *Fundamentals of Optics*, 3rd ed. (McGraw-Hill, New York, 1957), p. 468] with coefficients provided by Schott Glass Technologies, Inc. Indices might vary up to 0.003 from these values because of stresses in the NCG array.

[9] The NSOM itself is incorporated into a conventional microscope whose objective is used as the collection optic in this experiment. The conventional microscope is manufactured by Mitutoyo, and we use long working distance objectives of magnification $10\times$ (0.28 NA), $50\times$ (0.55 NA), and $100\times$ (0.7 NA).

[10] J. W. P. Hsu, Mark Lee, and B. S. Deaver, Rev. Sci. Instrum. **66**, 3177 (1995); Mark Lee, E. B. McDaniel, and J. W. P. Hsu, *ibid.* **67**, 1468 (1996).

[11] E. B. McDaniel and J. W. P. Hsu, J. Appl. Phys. **80**, 1085 (1996).

[12] A single cylindrical dielectric waveguide of the same dimension as the channel diameter is single mode for such a small index contrast. ''Modes'' in the text refer to those of the photonic crystal, not of single waveguides.

[13] A. Rosenberg, R. Tonucci, H.-B. Lin, and E. L. Shirley, Phys. Rev. B **54**, R5195 (1996).

[14] M. Plihal and A. A. Maradudin, Phys. Rev. B **44**, 8565 (1991).

[15] The maximum $|\mathbf{q}|$ collected by the 0.28 NA objective is 2.62×10^{-3} and 3.60×10^{-3} nm^{-1} for $\lambda=670$ and 488 nm, respectively.

[16] 0.55 NA corresponds to maximum $|\mathbf{q}|$ of 5.16×10^{-3} nm^{-1} ($\lambda=670$ nm) and 6.56×10^{-3} nm^{-1} ($\lambda=488$ nm). 0.7 NA corresponds to maximum $|\mathbf{q}|$ of 7.08×10^{-3} nm^{-1} ($\lambda=670$ nm) and 9.01×10^{-3} nm^{-1} ($\lambda=488$ nm).

[17] The NSOM data do not show evidence of the 3.5-nm (periodic) height variations seen in Fig. 1, most likely because the optical signal from these topographic features is much smaller than the signal associated with the mode structure of the crystal.

[18] Combined standard uncertainty is used here. The largest contribution arises from the determination of a constant offset, which was subtracted out at the beginning of each scan. This value, which was known to about ± 0.1 (68% confidence level) in the units of Fig. 4, results in a standard uncertainty of ± 0.08 in the ratios. The standard uncertainty due to random noise on the data is ± 0.05.

[19] Here the combined uncertainty of ± 0.04 is due primarily to the noise on the data. The offset uncertainty, which is the same as above, results in a standard uncertainty in the ratios of only ± 0.02.

[20] See, for example, the distance (10–90 % intensity change) from the central bright feature to the threefold sites in Fig. 3(f).

[21] G. W. Bryant, E. L. Shirley, L. S. Goldner, E. B. McDaniel, J. W. P. Hsu, and R. J. Tonucci (unpublished).

[22] C. J. Bouwkamp, Phillips Res. Rep. **5**, 321 (1950).

[23] Certain commercial equipment, instruments, or materials are identified in this paper to foster understanding. Such identification does not imply recommendation or endorsement by the National Institute of Standards and Technology, nor does it imply that the materials or equipment identified are necessarily the best available for the purpose.